Formation of ultrashort pulses via quantum interference between Stark-split atomic transitions in a hydrogenlike medium

V. A. Antonov,[1,2,3,*] Y. V. Radeonychev,[1,2,3] and Olga Kocharovskaya[2]

[1]*Institute of Applied Physics, Russian Academy of Sciences, 46 Ulyanov Street, Nizhny Novgorod, 603950, Russia*

[2]*Department of Physics and Astronomy and Institute for Quantum Studies and Engineering, Texas A&M University, College Station, TX 77843-4242, USA*

[3]*N. I. Lobachevsky State University of Nizhny Novgorod, 23 Gagarin Avenue, Nizhny Novgorod, 603950, Russia*

(Received 27 August 2013; published 27 November 2013)

We derive the analytical solution uncovering the origin of the ultrashort pulse formation from the resonant radiation in a hydrogenlike medium [Y. V. Radeonychev, V. A. Polovinkin, and O. Kocharovskaya, Phys. Rev. Lett. **105**, 183902 (2010)], which is a quantum interference of the atomic transitions from the ground to the first excited energy level split by an intense far-off-resonant laser field due to the instantaneous Stark effect into the periodically oscillating sublevels and interference of the resonantly scattered radiation with the incident one. The analytical solution shows that the pulses are almost bandwidth limited and can be produced in a wide range of parameters in excellent agreement with the more general numerical simulation. The experimental schemes to form few-femtosecond pulses from 122-nm radiation in atomic hydrogen as well as few-hundred-attosecond pulses from 13.74-nm radiation in a Li^{2+} medium are discussed.

DOI: 10.1103/PhysRevA.88.053849 PACS number(s): 42.65.Re, 42.65.Ky, 42.50.Gy, 42.50.Hz

I. INTRODUCTION

Few-femtosecond and attosecond pulses in various spectral regions are in demand for studies and control of the intra-atomic and intramolecular processes unfolding on the time scale of electronic motion [1–6]. The extremely short femtosecond pulses are currently generated by the ultrabroadband self-mode-locked laser systems [2,7,8], via the coherent summation of several-femtosecond laser pulses with different carrier wavelengths [9–11], as well as via the spectral broadening of laser radiation due to supercontinuum generation in crystals, fibers, and gases [12–14], and the stimulated Raman scattering of a bichromatic laser radiation [15–17]. The attosecond pulses are commonly produced via high-harmonic generation of laser radiation in gases due to ionization and subsequent recombination of the detached electron with the parent ion [18–20]. A possibility to generate atto- and zeptosecond pulses via reflection of an ultraintense laser pulse from an overdense plasma surface attracts growing attention [21–23].

Recently, we proposed an approach to extremely short femto- and attosecond pulse formation via transformation of a resonant radiation in a hydrogenlike medium irradiated by a far-off-resonant laser field [24–28]. The pulses are produced due to ultrabroadband atomic response to the resonant radiation under the action of a strong low-frequency (LF) laser field, which causes time-dependent Stark splitting of the excited atomic energy levels and tunnel ionization from the excited states. We reported the possibility to form almost bandwidth-limited few-femtosecond pulses in atomic hydrogen as well as few-hundred-attosecond pulses in Li^{2+} plasma with peak intensity of the pulses appreciably exceeding the intensity of the incident resonant radiation. All the previous results were based on numerical simulations.

In this paper, we derive the analytical solution describing the pulse formation from a resonant high-frequency (HF) radiation in a hydrogenlike medium due to instantaneous Stark splitting of the first excited energy level by a far-off-resonant LF laser field [24,26]. We show that the pulses are produced due to the dual-type interference: (i) quantum interference of atomic transitions from the ground to the Stark-split first excited atomic energy level, and (ii) interference of the resonantly scattered radiation with the incident one. The analytical solution takes into account the space-time dependence of the linear Stark splitting of the excited energy level as well as the constant shift and broadening of the produced sublevels due to the quadratic Stark effect and ionization from the excited states, induced by the LF field, respectively. The solution implies a small energy transfer from the incident resonant HF radiation into the generated sidebands. In the wide range of parameter values the analytical solution is found to be in excellent agreement with the numerical calculations within the more comprehensive model [25,27] accounting for the propagation effects in an optically deep medium as well as the nonlinear space-time dependences of both the Stark shifts and splitting of the excited atomic energy levels and the ionization rates from them.

II. ANALYTICAL SOLUTION

Let us consider propagation of a HF radiation through a gas of hydrogenlike atoms. The incident HF radiation is linearly polarized and monochromatic. At the input to the medium, $z = 0$, it has a form

$$\vec{E}_{\rm inc}(t) = \tfrac{1}{2}\vec{x}_0 E_0 \exp\{-i\omega t\} + \text{c.c.}, \qquad (1)$$

where E_0 is the amplitude, ω is the angular frequency, and c.c. stands for complex conjugation. The HF radiation (1) is near resonant to the atomic transition between the ground and the first excited energy levels $n = 1 \leftrightarrow n = 2$ (n is the principal quantum number).

*Corresponding author: antonov@appl.sci-nnov.ru

The medium is simultaneously irradiated by an intense low-frequency (LF) laser field

$$\vec{E}_{LF}(z,t) = \tfrac{1}{2}\vec{x}_0 E_C \exp\{-i\,\Omega(t - z/c)\} + \text{c.c.}, \qquad (2)$$

which is far off resonant to all the transitions involving the populated atomic states and propagates through the medium without substantial distortions. In (2) E_C is the amplitude of the LF field, Ω is its angular frequency, and c is the speed of light in vacuum. Since the HF and the LF radiation are polarized in the same direction, $\vec{E}_{\text{inc}} || \vec{E}_{LF} || \vec{x}_0$, their polarizations are not changed during propagation through the isotropic medium. Therefore, the vector notations can be omitted.

Propagation of the HF radiation E_{HF} through the medium is described by the wave equation

$$\frac{\partial^2 E_{HF}}{\partial z^2} - \frac{1}{c^2}\frac{\partial^2 E_{HF}}{\partial t^2} = \frac{4\pi}{c^2}\frac{\partial^2 P}{\partial t^2}, \qquad (3)$$

where z is the propagation coordinate and P is the induced HF polarization of the medium. Since the characteristic scale of spatial evolution of the HF radiation in a gas is much larger than the radiation wavelength, after the change of independent variables $t \to \tau \equiv t - z/c$, the wave equation (3) can be reduced to

$$\frac{\partial E_{HF}}{\partial z} = -\frac{2\pi}{c}\frac{\partial P}{\partial \tau}. \qquad (4)$$

Equation (4) implies the slowly evolving wave approximation [29,30], $|\frac{\partial E_{HF}}{\partial z}| \ll \frac{1}{c}|\frac{\partial E_{HF}}{\partial \tau}|$. Within the additional approximation of slowly varying envelope, $E_{HF}(z,\tau) = \frac{1}{2}\tilde{E}_{HF}(z,\tau)\exp\{-i\omega\tau\} + \text{c.c.}$, $P(z,\tau) = \frac{1}{2}\tilde{P}(z,\tau)\exp\{-i\omega\tau\} + \text{c.c.}$, $|\partial\tilde{E}_{HF}/\partial\tau| \ll \omega$, $|\partial\tilde{P}/\partial\tau| \ll \omega$, $|\partial\tilde{E}_{HF}/\partial z| \ll \omega/c$, and $|\partial\tilde{P}/\partial z| \ll \omega/c$; Eq. (4) has the solution

$$\tilde{E}_{HF}(z,\tau) = \tilde{E}_{HF}(0,\tau) + i\frac{2\pi\omega}{c}\int_0^z \tilde{P}(z',\tau)dz'. \qquad (5)$$

The HF polarization of the medium is determined by the resonant atomic transition $n = 1 \leftrightarrow n = 2$ and consists of the contributions corresponding to the transitions from the ground state $|1\rangle = |100\rangle$ to the excited states $|2\rangle = (|200\rangle + |210\rangle)/\sqrt{2}$ and $|3\rangle = (|200\rangle - |210\rangle)/\sqrt{2}$ (the numerals $|nlm\rangle$ label principal, orbit, and magnetic quantum numbers, respectively) representing the sublevels of the first excited atomic energy level $n = 2$ in the presence of a LF electric field [24–28,31]:

$$\tilde{P}(z,\tau) = 2Nd_{tr}\{a_{21} - a_{31}\}, \qquad (6)$$

where a_{21} and a_{31} are the slowly varying envelopes of the atomic coherences ρ_{21} and ρ_{31} induced at the transitions $|1\rangle \leftrightarrow |2\rangle$ and $|1\rangle \leftrightarrow |3\rangle$, respectively, $\rho_{21} = a_{21}\exp\{-i\,\omega\tau\}$, $\rho_{31} = a_{31}\exp\{-i\,\omega\tau\}$, N is the concentration of atoms, and $d_{tr} = 2^7 e r_B/(3^5 Z)$ is the dipole moment of the resonant transitions (e is the charge of electron, r_B is the Bohr radius, Z is the atomic number). Equation (6) implies that the excited states $|2\rangle$ and $|3\rangle$ are not populated: $\rho_{22} = 0$, $\rho_{33} = 0$. We also assume that most of the atoms remain unexcited during the interaction time, $\rho_{11} = 1$, similar to the papers [24–27].

In the following we consider a LF field whose amplitude meets the inequality $F_c \leqslant 0.05$, where $F_c = (2/Z)^3 E_c/E_A$ is the LF field strength in the excited-state atomic units (for $n = 2$) [32], and $E_A = \frac{m_e^2 e^5}{\hbar^4} \cong 5.14 \times 10^9$ V/cm is the atomic unit of the electric field (m_e is the mass of the electron, $\hbar$ is Planck's constant). Due to the linear Stark effect, the LF field splits the first excited atomic energy level $n = 2$ into the sublevels $|2\rangle$ and $|3\rangle$ oscillating in time and space along with the instantaneous LF field strength (2), Fig. 1. Variation of the instantaneous positions of these sublevels leads to the space-time modulation of frequencies of the atomic transitions $|1\rangle \leftrightarrow |2\rangle$ and $|1\rangle \leftrightarrow |3\rangle$ resonant to the HF radiation:

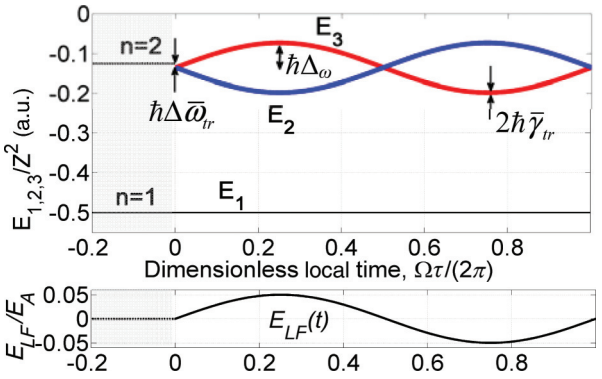

FIG. 1. (Color online) Top panel: the relevant energy levels of a hydrogenlike atom: The bold red and blue lines represent sublevels $|2\rangle$ and $|3\rangle$ of the first excited energy level $n = 2$, the straight black line corresponds to the ground level $|1\rangle$, $n = 1$. Bottom panel: the low-frequency field strength causing oscillation of the sublevels $|2\rangle$ and $|3\rangle$ (shown on the top panel) in space and time with the amplitude $\hbar\Delta_\omega$, as well as the constant shift $\hbar\Delta\bar{\omega}_{tr}$ and constant broadening $2\hbar\bar{\gamma}_{tr}$ of these sublevels.

$$\omega_{21}(z,\tau) = \bar{\omega}_{tr} - \Delta_\omega\cos(\Omega\tau),$$
$$\omega_{31}(z,\tau) = \bar{\omega}_{tr} + \Delta_\omega\cos(\Omega\tau), \qquad (7)$$

where $\Delta_\omega = \frac{3}{8}\frac{m_e e^4 Z^2}{\hbar^3}F_C$ [32]. The average frequency of these transitions $\bar{\omega}_{tr}$ is shifted with respect to the frequency of the unperturbed transition $n = 1 \leftrightarrow n = 2$ due to the quadratic Stark effect [32]: $\bar{\omega}_{tr} = \frac{3}{8}\frac{m_e e^4 Z^2}{\hbar^3}(1 - \frac{7}{4}F_C^2)$. The LF field also causes an increase in the decoherence rates of atomic transitions via ionization from the excited states: $\bar{\gamma}_{tr} = \gamma_0 + \frac{\bar{w}_{ion}^{(2;3)}}{2}$, where $\gamma_0 = \gamma_{\text{coll}} + \frac{A}{2}$, γ_{coll} is the collisional broadening, A is the spontaneous decay rate, and $\bar{w}_{ion}^{(2;3)}$ is the ionization rate from either $|2\rangle$ or $|3\rangle$ state, averaged over the LF-field cycle, $\bar{w}_{ion}^{(2;3)} = \frac{m_e e^4 Z^2}{16\hbar^3}\sqrt{\frac{3F_c}{\pi}}[(\frac{4}{F_c})e^{+3} + (\frac{4}{F_c})^3 e^{-3}]\exp\{-\frac{2}{3F_c}\}$ [32]. The space-time dependences of the quadratic Stark shifts and the excited-state ionization rates can be disregarded as far as their peak values are significantly smaller than the frequency of the LF field, $\frac{21}{16}\frac{m_e e^4 Z^2}{\hbar^3}F_c^2 \ll \Omega$, $\frac{m_e e^4 Z^2}{2\hbar^3 F_c}\exp\{3 - \frac{2}{3F_c}\} \ll \Omega$ [33]. The latter inequality implies that the ionization-broadened atomic resonances are narrow as compared to the frequency of the LF field, $\bar{\gamma}_{21,31} \ll \Omega$.

Equations for the amplitudes of the atomic coherences a_{21} and a_{31} take the form

$$\frac{\partial a_{21}}{\partial\tau} + [i\{\bar{\omega}_{tr} - \omega - \Delta_\omega\cos(\Omega\tau)\} + \bar{\gamma}_{tr}]a_{21} = i\frac{d_{tr}\tilde{E}_{HF}}{2\hbar},$$
$$\frac{\partial a_{31}}{\partial\tau} + [i\{\bar{\omega}_{tr} - \omega + \Delta_\omega\cos(\Omega\tau)\} + \bar{\gamma}_{tr}]a_{31} = -i\frac{d_{tr}\tilde{E}_{HF}}{2\hbar}, \qquad (8)$$

where the rotating-wave approximation is used.

According to the results of the numerical study presented in [24,26], the ultrashort pulses can be produced from the incident HF radiation in an infinitely thin medium, and increase of the medium thickness leads just to an increase of the peak amplitude of the pulses (due to increased intensity of the generated sidebands) at the cost of a slight increase of the pulse duration (because of phase mismatching of the sidebands). Therefore, in order to derive the analytical solution, we assume that the length of the medium is small enough, such that the incident spectral component dominates over the generated sidebands. In this case, the resonant atomic response can be calculated accounting only for the coherent scattering of the incident HF radiation and neglecting rescattering of the generated sidebands. Substitution of (1) into (8) and neglect of rescattering of the HF radiation, i.e., $E_{HF}(z,\tau) \approx E_{\rm inc}(\tau)$, leads to the solution

$$\begin{aligned} a_{21}(\tau) &= i\frac{d_{tr}E_0}{2\hbar\bar{\gamma}_{tr}}\exp\{iP_\omega\sin(\Omega\tau)\} \\ &\quad\times\sum_{n=-\infty}^{\infty}\frac{J_n(P_\omega)\exp\{-in\Omega\tau\}}{i(\bar{\omega}_{tr}-\omega-n\Omega)+\bar{\gamma}_{tr}}, \\ a_{31}(\tau) &= -i\frac{d_{tr}E_0}{2\hbar\bar{\gamma}_{tr}}\exp\{-iP_\omega\sin(\Omega\tau)\} \\ &\quad\times\sum_{n=-\infty}^{\infty}\frac{J_n(P_\omega)\exp\{in\Omega\tau\}}{i(\bar{\omega}_{tr}-\omega+n\Omega)+\bar{\gamma}_{tr}}, \end{aligned} \tag{9}$$

where $P_\omega \equiv \Delta_\omega/\Omega$ is the modulation index of the atomic transition frequencies [24,26], $J_n(P_\omega)$ is the Bessel function of the first kind of order n. The atomic coherences are most effectively excited if the incident HF radiation (1) is tuned to resonance with the corresponding transitions $|1\rangle\leftrightarrow|2\rangle$ and $|1\rangle\leftrightarrow|3\rangle$ shifted by the LF field due to the quadratic Stark effect, or detuned from the Stark-shifted resonance by a multiple of the LF field frequency. Thus, in the following we consider the case $\omega = \bar{\omega}_{tr} + m_*\Omega$, where $m_* = 0, \pm1, \pm2, \cdots$. Since $\Omega \gg \bar{\gamma}_{21,31}$, we obtain

$$\begin{aligned} a_{21}(\tau) &= (-1)^{m_*}i\frac{d_{tr}E_0}{2\hbar\bar{\gamma}_{tr}}J_{m_*}(P_\omega)\exp\{im_*\Omega\tau\} \\ &\quad\times\exp\{iP_\omega\sin(\Omega\tau)\}, \\ a_{31}(\tau) &= -i\frac{d_{tr}E_0}{2\hbar\bar{\gamma}_{tr}}J_{m_*}(P_\omega)\exp\{im_*\Omega\tau\} \\ &\quad\times\exp\{-iP_\omega\sin(\Omega\tau)\}. \end{aligned} \tag{10}$$

Integration of (5), taking (6) and (10) into account, gives the amplitude of the HF radiation at the output of the medium, $z = L$, in the form

$$\begin{aligned} &\tilde{E}_{HF}(t) \\ &= E_0 - E_0J_{m_*}(P_\omega)\frac{4\pi Nd_{tr}^2L}{\hbar\bar{\gamma}_{tr}}\frac{\omega}{c}\exp\{im_*\Omega t\} \\ &\quad\times\begin{cases}\sum_{n=-\infty}^{+\infty}J_{2n}(P_\omega)\exp\{-i2n\Omega t\}, & m_* = 2k, \\ \sum_{n=-\infty}^{+\infty}J_{2n+1}(P_\omega)\exp\{-i(2n+1)\Omega t\}, & m_* = 2k+1, \end{cases} \end{aligned} \tag{11}$$

where L is the propagation length and the relation $J_{-n}(P_\omega) = (-1)^nJ_n(P_\omega)$ is taken into account. The upper row in (11) corresponds to the incident HF radiation (1) tuned to atomic resonance, $m_* = 0$, or shifted from it by an even number of frequencies of the LF field, $m_* = \pm2, \pm4, \ldots$. The lower row corresponds to the incident HF radiation (1) detuned from the resonance by an odd number of the LF field frequencies, $m_* = \pm1, \pm3, \ldots$. The reverse transformation from the slowly varying amplitude $\tilde{E}_{HF}(t)$ to the rapidly oscillating HF field $E_{HF}(t) = \frac{1}{2}\tilde{E}_{HF}(t)\exp\{-i\omega t\} + \text{c.c.}$ results in

$$\begin{aligned} E_{HF}(t) &= E_0\cos\{(\bar{\omega}_{tr}+m_*\Omega)t\} \\ &\quad - J_{m_*}(P_\omega)E_0\frac{4\pi Nd_{tr}^2L}{\hbar\bar{\gamma}_{tr}}\frac{\omega}{c} \\ &\quad\times\begin{cases}\cos\{P_\omega\sin(\Omega t)\}\cos\{\bar{\omega}_{tr}t\}, & m_* = 2k, \\ -\sin\{P_\omega\sin(\Omega t)\}\sin\{\bar{\omega}_{tr}t\}, & m_* = 2k+1. \end{cases} \end{aligned} \tag{12}$$

While the coherences at each of the resonantly excited atomic transitions $|1\rangle\leftrightarrow|2\rangle$ and $|1\rangle\leftrightarrow|3\rangle$ are frequency modulated, Eq. (10), the resonantly scattered radiation [right-hand side of Eq. (12) after subtraction of the incident radiation (1)] is purely amplitude modulated. This is the manifestation of quantum interference of the resonant atomic transitions contributing in antiphase to each other to the overall polarization of the medium (6). However, this amplitude modulation of the scattered radiation does not correspond yet to formation of the ultrashort pulses; the pulses arise only for the scattered radiation coherently superposed to the incident one (12). The quantum interference leads to specific alignment of phases of the generated sidebands. As follows from (11), if the incident HF radiation is tuned to resonance or detuned from it by an even number of frequencies of the LF field, $m_* = 0, \pm2, \pm4, \ldots$, the produced spectral components on both sides from the resonance have the same phases, since $J_{-2n}(P_\omega) = J_{2n}(P_\omega)$. In the case of the incident HF radiation detuned from the resonance by an odd number of frequencies of the LF field, $m_* = \pm1, \pm3, \ldots$, the phases of the spectral components on different sides from the resonance are shifted by π from each other (11), since $J_{-(2n+1)}(P_\omega) = -J_{2n+1}(P_\omega)$. In order to produce the phase-matched sidebands, hereinafter we consider the former case, $m_* = 0, \pm2, \pm4, \ldots$. The phases of the generated spectral components on each side from the resonance are determined by the sign of Bessel functions and depend on the modulation index $P_\omega \equiv \Delta_\omega/\Omega$. Variation of the Bessel functions of even orders J_{2n} vs the modulation index P_ω is plotted in Fig. 2. If $P_\omega < \nu_0^{(1)}$, where $\nu_0^{(1)} \cong 2.40$ is the first root of the equation $J_0(\nu) = 0$, all the Bessel functions are positive. In the case $\nu_0^{(1)} < P_\omega < \nu_2^{(1)}$, where $\nu_2^{(1)} \cong 5.14$ is the first root of the equation $J_2(\nu) = 0$, the Bessel functions are positive except the zeroth order. In the case $\nu_0^{(2)} < P_\omega < \nu_4^{(1)}$, where $\nu_0^{(2)} \cong 5.52$ is the second root of the equation $J_0(\nu) = 0$ and $\nu_4^{(1)} \cong 7.59$ is the first root of the equation $J_4(\nu) = 0$, the Bessel functions are positive except those of orders ±2.

III. DISCUSSION OF THE POSSIBILITIES FOR EXPERIMENTAL REALIZATION

Henceforth, we consider the possibilities of ultrashort pulse formation from the incident HF radiation in the cases $\nu_0^{(1)} < P_\omega < \nu_2^{(1)}$ and $\nu_0^{(2)} < P_\omega < \nu_4^{(1)}$, and discuss the experimental

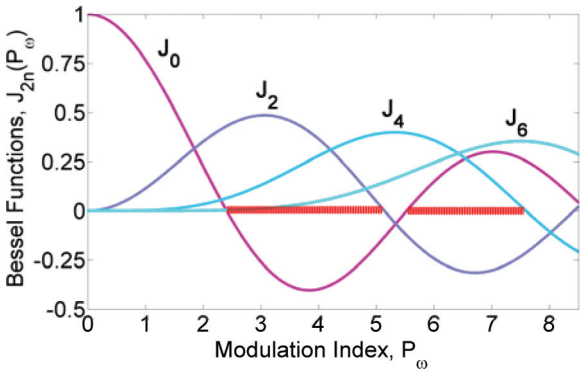

FIG. 2. (Color online) Bessel functions of the first kind J_{2n} of even orders vs the modulation index P_ω. The dashed red lines on the horizontal axis show the intervals $\nu_0^{(1)} < P_\omega < \nu_2^{(1)}$ and $\nu_0^{(2)} < P_\omega < \nu_4^{(1)}$, suitable for the ultrashort pulse formation, see (13), (14) and (15), (16).

realization in atomic hydrogen as well as in Li^{2+} plasma. In the case $\nu_0^{(1)} < P_\omega < \nu_2^{(1)}$, the generated sidebands are *in phase* with the incident radiation, if it is tuned to resonance with the atomic transition, shifted by the LF field via the quadratic Stark effect, i.e., if $\omega = \bar{\omega}_{tr}, m_* = 0$. According to (12), attenuation of the output spectral component at the frequency of the incident HF radiation to the level of the generated sidebands results in the output radiation in the form

$$E_{HF}(L,t) = E_0 A_0[-J_0(P_\omega)][\delta + \cos\{P_\omega \sin(\Omega t)\}]\cos(\omega t), \tag{13}$$

where $A_0 = \frac{4\pi N d_{tr}^2 L}{\hbar \bar{\gamma}_{tr}} \frac{\omega}{c}$ is the dimensionless coefficient [$A_0 J_0(P_\omega)$ corresponds to the ratio of the amplitude of the generated sidebands to the amplitude of the incident HF radiation], $A_0 \ll 1$; δ is the coefficient, which determines the optimal level of attenuation of the incident spectral component (the spectral component at the frequency of the incident HF radiation ω), $\delta = -J_0(P_\omega) + J_2(P_\omega)$ if $2.40 \leqslant P_\omega \leqslant 4.20$ and $\delta = -J_0(P_\omega) + J_4(P_\omega)$ if $4.20 < P_\omega \leqslant 5.14$. In concordance with (11), Fourier decomposition of the output radiation (13) has the form

$$\begin{aligned} E_{HF}(L,t) = {} & E_0 A_0[-J_0(P_\omega)] \\ & \times \left([\delta + J_0(P_\omega)] + \sum_{n\neq 0} J_{2n}(P_\omega) \exp\{-i2n\Omega t\} \right) \\ & \times \exp\{-i\omega t\} + \text{c.c.} \end{aligned} \tag{14}$$

Since the value of the modulation index satisfies the inequality $\nu_0^{(1)} < P_\omega < \nu_2^{(1)}$, the Bessel function of zeroth order is negative, $J_0(P_\omega) < 0$, while all the other Bessel functions of even orders are positive, $J_n(P_\omega) > 0$, $n = \pm 2, \pm 4, \ldots$. According to (14), this means that the resonant interaction of the HF radiation with the atoms leads to (i) absorption of the incident radiation at the frequency ω and (ii) generation of the combinational spectral components at the frequencies $\omega_{2n} = \omega + 2n\Omega$, $n = \pm 1, \pm 2, \ldots$ *in phase* to the incident radiation. Constructive interference of the generated sidebands with each other and with the incident HF radiation leads to formation of a train of *bandwidth-limited* pulses.

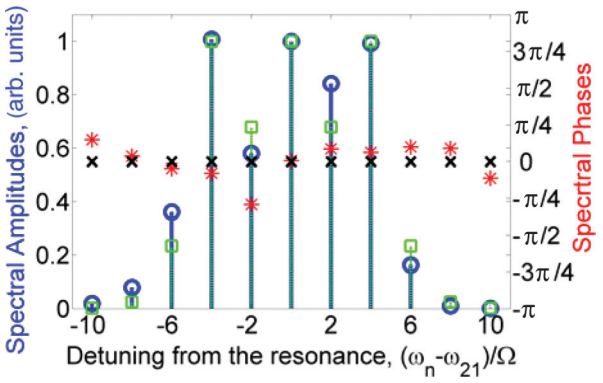

FIG. 3. (Color online) Fourier transform of the 122.1-nm VUV radiation E_{HF} propagated through the medium of atomic hydrogen, $N_H = 10^{17}$ cm^{-1}, $L = 0.7$ mm, along with the 10.65-μm CO_2-laser field with intensity $I_{CO2} = 1.4 \times 10^{12}$ W/cm^2, providing $P_\omega = 4.45$. The amplitudes and phases of the spectral components calculated analytically (14) are shown by green squares and black crosses, respectively, while the numerical results taking into account the space-time dependencies of both the nonlinear Stark effect and the excited-state ionization rates [25] are shown by blue circles and red stars, labeling amplitudes and phases of the spectral components, correspondingly. The "0" spectral component at the frequency of the incident VUV radiation is attenuated to the level of the generated sidebands.

Let us consider the experimental realization of the above regime in atomic hydrogen simultaneously irradiated by 122.1-nm vacuum ultraviolet (VUV) radiation produced, e.g., via nonlinear upconversion of a visible laser field [34,35], and a CO_2-laser radiation at 10.65 μm of intensity $I_{CO2} = 1.4 \times 10^{12}$ W/cm^2 [36]. The CO_2-laser radiation splits and shifts the $n = 1 \leftrightarrow n = 2$ atomic transition line due to the Stark effect, providing the value of modulation index $P_\omega = 4.45$, while the VUV radiation resonantly excites the atomic coherences. In Fig. 3 we compare the analytically calculated spectrum (14) of the output VUV radiation (13) to the result of numerical solution, obtained for concentration of atomic hydrogen $N_H = 10^{17}$ cm^{-1} and propagation length $L = 0.7$ mm. Unlike the analytical solution, the numerical results are obtained for an optically deep medium within the model [25,27] taking into account the propagation effects as well as the space-time dependencies of both the instantaneous nonlinear Stark effect and tunnel ionization rates from the excited atomic states. According to the results of numerical calculation, for the chosen parameter values the amplitudes of the generated sidebands become comparable to the amplitude of the incident HF radiation. However, as seen from Fig. 3, the analytical solution is in excellent agreement with the numerical one. The agreement becomes even more striking in Fig. 4, where the analytically calculated intensity of the output VUV radiation $I \sim |\tilde{E}_{HF}|^2$ is compared to the numerical solution for the square of the output VUV radiation strength E_{HF}^2. As seen in Fig. 4, the resonant interaction of the VUV radiation with the atoms and attenuation of the incident VUV spectral component to the level of the generated sidebands result in formation of a train of the ultrashort bandwidth-limited pulses. The pulse duration and repetition period are $\tau_{\text{pulse}} = 2.6$ fs and $T = 17.8$ fs, respectively. The peak intensity of the pulses

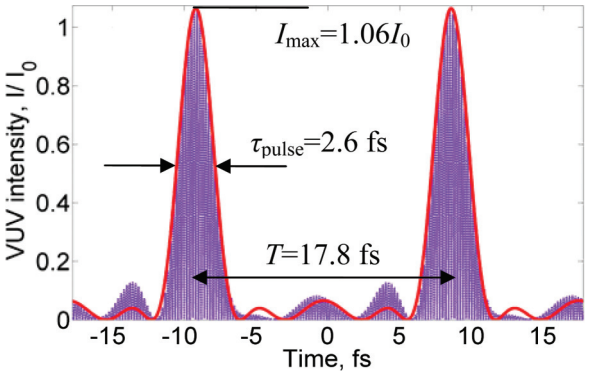

FIG. 4. (Color online) Intensity $I \sim |E_{HF}|^2$ of the output VUV radiation normalized to the incident VUV intensity I_0, corresponding to the spectrum in Fig. 3. The bold red curve shows the analytical solution (13). The dashed lavender curve corresponds to the numerical results [25]. The produced pulses are bandwidth limited.

is $I_{max} = 1.06I_0$, where I_0 is the incident VUV intensity. The efficiency of conversion of the incident VUV radiation into the pulses equals 19%. The conversion efficiency is much larger if the incident spectral component is not attenuated, at the cost of increased pulse duration and slightly degraded pulse shape. As an example, the pulses produced at a medium length increased to $L = 1.8$ mm *without* attenuation of the incident component of the VUV spectrum are shown in Fig. 5. The peak intensity of the pulses is $I_{max} = 2.9I_0$, while the conversion efficiency of the VUV radiation reaches 76%; the pulse duration equals $\tau_{pulse} = 3.2$ fs.

Order of magnitude shorter pulses can be produced from the extreme ultraviolet (XUV) radiation in the medium of hydrogenlike Li^{2+} ions. Let us discuss the possibilities of the XUV attosecond pulse formation in the case where the modulation index meets the inequality $\nu_0^{(2)} < P_\omega < \nu_4^{(1)}$. In this case, the sidebands are generated *in phase* with the incident radiation, if it is detuned from the atomic resonance (shifted by the LF field due to the quadratic Stark effect) by the doubled frequency of the LF field, $\omega = \bar{\omega}_{tr} \pm 2\Omega$. After propagation through an optically thin medium and attenuation of the output spectral component at the frequency of the incident XUV

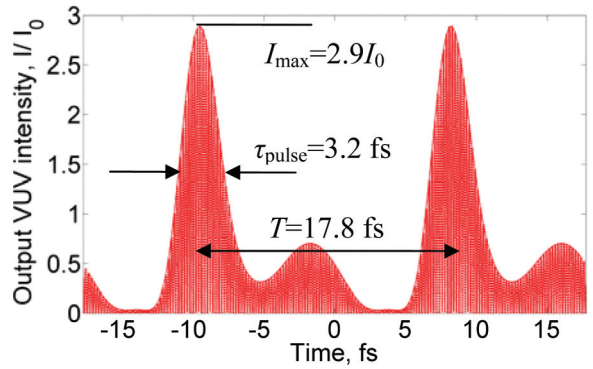

FIG. 5. (Color online) Intensity $I \sim |E_{HF}|^2$ of the output VUV radiation, normalized to the incident VUV intensity I_0. The propagation distance in atomic hydrogen is $L = 1.8$ mm; the other parameters are the same as in Figs. 3 and 4. The pulses are produced *without attenuation* of any component of the output VUV spectrum.

radiation to the level of the generated sidebands, in accordance with (12) the XUV radiation acquires the form

$$E_{HF}(L,t) = E_0 A_0[-J_2(P_\omega)](\delta\cos(\omega t) + \cos\{P_\omega \sin(\Omega t)\} \times \cos[(\omega \mp 2\Omega)t]), \quad (15)$$

where $A_0 = \frac{4\pi N d_{tr}^2 L}{\hbar \bar{\gamma}_{tr}} \frac{\omega}{c}$; "$-$" and "$+$" correspond to the cases $\omega = \bar{\omega}_{tr} \pm 2\Omega$, respectively. The coefficient δ determines the optimal level of attenuation of the output spectral component at the frequency of the incident XUV radiation; $\delta = -J_2(P_\omega) + J_4(P_\omega)$ if $5.52 \leqslant P_\omega \leqslant 6.42$ and $\delta = -J_2(P_\omega) + J_6(P_\omega)$ if $6.42 < P_\omega \leqslant 7.59$. In compliance with (11), Fourier decomposition of the output XUV radiation has the form

$$E_{HF}(L,t) = E_0 A_0[-J_2(P_\omega)] \times \left([\delta + J_2(P_\omega)] + \sum_{n\neq 0} J_{2(n\pm 1)}(P_\omega)\exp\{-i2n\Omega t\}\right) \times \exp\{-i\omega t\} + \text{c.c.} \quad (16)$$

In the considered case $\nu_0^{(2)} < P_\omega < \nu_4^{(1)}$ the Bessel functions of orders ± 2 are negative, $J_{\pm 2}(P_\omega) < 0$, while all the rest of the Bessel functions of even orders are positive, $J_n(P_\omega) > 0$ for $n = 0, \pm 4, \pm 6, \ldots$. According to (16), this means that (i) the incident XUV radiation is absorbed, while (ii) the spectral components are generated at the frequencies $\omega_{\pm 2n} = \bar{\omega}_{tr} \pm 2n\Omega$ in phase with the incident radiation except the component at the frequency $\omega_{\mp 2} = \bar{\omega}_{tr} \mp 2\Omega$ (corresponding to $\omega = \bar{\omega}_{tr} \pm 2\Omega$), which is antiphased to the rest of the components of the output spectrum. The constructive interference of the majority of the output spectral components with each other and with the incident XUV radiation results in formation of a train of attosecond pulses, while the role of the antiphased component is limited to reduction of the pulse peak intensity and increase of the pulse pedestal. Surprisingly, the duration of the produced pulses is even a bit smaller than the corresponding bandwidth-limited value, which can be achieved via tuning the antiphased component in phase with the rest of the components of the output spectrum.

In the case of Li^{2+} medium, the regime $\nu_0^{(2)} < P_\omega < \nu_4^{(1)}$ can be achieved using the LF field with the wavelength >1.5 μm. Decrease of the LF wavelength below 1.5 μm is not admissible, since in order to get $P_\omega > \nu_0^{(2)}$ ($P_\omega \equiv \Delta_\omega/\Omega$, $\Delta_\omega \sim E_C$) it would require increase of the LF field strength E_C above the threshold of rapid atomic ionization from the excited states $|2\rangle$ and $|3\rangle$, $\bar{w}_{ion}^{(2;3)} \geqslant \Omega$, causing mismatch of the phases of the generated sidebands. The optimal wavelength of the incident XUV radiation, detuned from the atomic resonance (shifted by the LF field due to the quadratic Stark effect) by $\pm 2\Omega$, depends on the LF field frequency and strength and varies in the range 13.3 nm $< \lambda_{XUV} <$ 13.8 nm. The available XUV radiation sources include the Ni-like Ag and Cd x-ray lasers, providing radiation at 13.9 and 13.2 nm, respectively [37,38], the H-like Li x-ray laser [39] radiating at 13.5 nm, and the tunable XUV free-electron lasers (FEL) [40–42]. In the following we consider propagation of the 13.74-nm XUV radiation of a FEL through the medium of Li^{2+} ions with the ion concentration $N_{Li2+} = 10^{18}$ cm^{-1} and length $L = 80$ μm along with 2-μm laser radiation of intensity

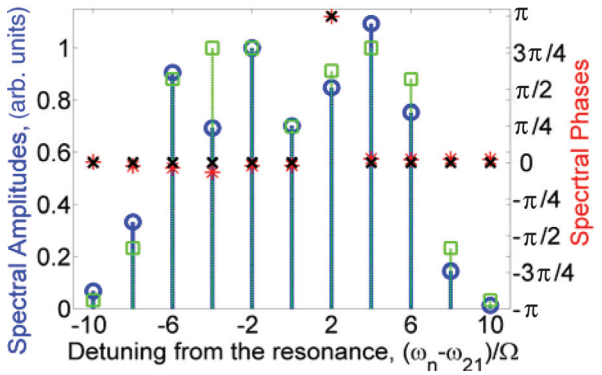

FIG. 6. (Color online) Fourier transform of the 13.74-nm XUV radiation E_{HF} after propagation through the medium of Li^{2+} ions, $N_{Li2+} = 10^{18}$ cm^{-1}, $L = 80$ μm, along with the 2-μm laser field with intensity $I_{2\mu m} = 7.2 \times 10^{14}$ W/cm^2, providing $P_\omega = 6.3$. The "-2"spectral component at the frequency of the incident XUV radiation is attenuated to the level of the generated sidebands. The amplitudes and phases of the spectral components calculated analytically (16) are shown by the green squares and the black crosses, correspondingly, while the results of numerical solution taking into account the space-time dependencies of both the nonlinear Stark effect and the excited-state ionization rates [25] are shown by the blue circles and the red stars, labeling the amplitudes and phases of the spectral components, respectively.

$I_{2\mu m} = 7.2 \times 10^{14}$ W/cm^2 [43–45], providing the value of modulation index $P_\omega = 6.3$. After the optimal attenuation of the incident XUV spectral component via reflection from a narrowband frequency-tunable Si:Mo mirror [46,47] the XUV spectrum acquires the form shown in Fig. 6. This spectrum corresponds to formation of the attosecond pulse train shown in Fig. 7. The duration and repetition period of the produced pulses equal $\tau_{pulse} = 340$ as and $T = 3.33$ fs, respectively, while the pulse peak intensity is $I_{max} = 0.5I_0$, where I_0 is the incident XUV radiation intensity. Change of the phase of the "$+2$" antiphased XUV spectral component in Fig. 6 by π will result in formation of the bandwidth-limited pulses shown in Fig. 8. In this case, the pulse duration is $\tau_{pulse} = 380$ as, while the peak intensity of the produced pulses rises to $I_{max} = 0.9I_0$. The efficiency of conversion of the XUV radiation into the pulse

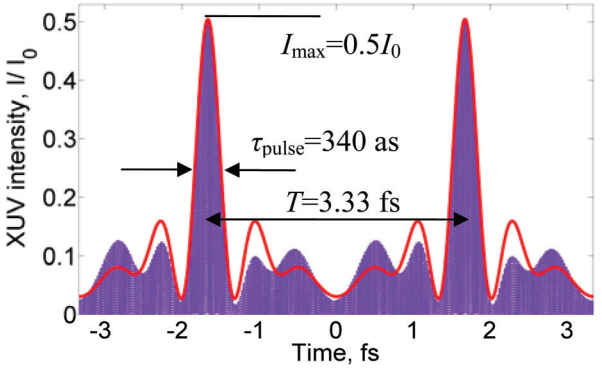

FIG. 7. (Color online) Normalized intensity $I \sim |E_{HF}|^2$ of the output XUV radiation corresponding to the spectrum in Fig. 6. The bold red curve shows the analytically calculated envelope (15), while the dashed lavender curve shows the numerical results [25].

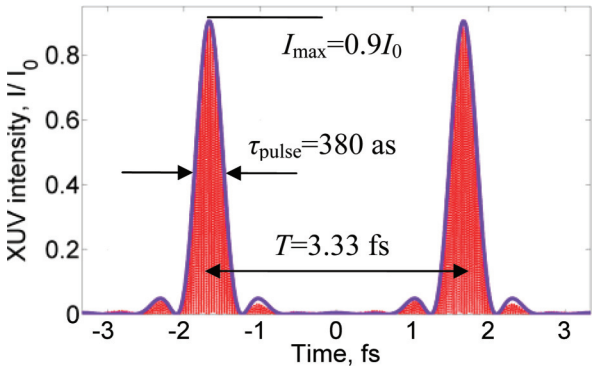

FIG. 8. (Color online) Bandwidth-limited attosecond XUV pulses produced via shifting the phase of the "$+2$" output XUV spectral component, Fig. 6, by π. Intensity of the XUV radiation $I \sim |E_{HF}|^2$ is normalized to the incident XUV intensity I_0. The bold lavender curve corresponds to the analytically calculated envelope, while the dashed red curve represents the numerical results [25].

trains in Figs. 7 and 8 equals 12%. As seen from Figs. 6–8, the analytical solution is in excellent agreement with the numerical calculation within the more general model from [25,27]. It is worth noting that the femtosecond duration of the incident XUV radiation pulse provided by the state-of-the-art FEL [41,42] might allow generation of a *single* XUV attosecond burst, as shown in our recent paper [28].

The above investigation shows that the discussed approach to formation of ultrashort pulses can be realized in a wide range of optical depths of the medium and amplitudes of the incident HF radiation (as far as the incident HF spectral component dominates over the generated sidebands and most of the atoms remain unexcited during the interaction time). The frequency of the LF field is restricted from below by the linewidth of ionization-broadened resonant atomic transitions and from above by the frequencies of atomic transitions involving the populated states. The LF field amplitude may vary in the wide range, determined by the inequalities $\nu_0^{(1)} < P_\omega < \nu_2^{(1)}$ and $\nu_0^{(2)} < P_\omega < \nu_4^{(1)}$, where $\nu_0^{(1)} \cong 2.40$ and $\nu_4^{(1)} \cong 7.59$, corresponding to variation of intensity of the LF field by an order of magnitude. The frequency of the incident HF radiation should be adjusted with the accuracy on the order of the linewidth of the ionization-broadened atomic resonance.

In the case of pulse formation from VUV radiation in atomic hydrogen, most of the atoms remain in the ground state during the interaction time, and only a negligibly small fraction of atoms is ionized from the excited states by the LF field and produces free electrons. As a result, the plasma dispersion is unimportant and can be disregarded. In the medium of Li^{2+} ions, instead, the role of plasma dispersion is significant. It is assumed above that the phase velocity of the LF field equals the speed of light in vacuum, c. While this is a reasonable approximation for a rarefied neutral gas, in a doubly ionized plasma characterized by nonresonant dielectric permittivity $\varepsilon_p = 1 - \omega_p^2/\omega^2$, where $\omega_p^2 = 4\pi N_e e^2/m_e$, N_e is the concentration of free electrons, and the phase velocity of the LF field increases to the value $c_{LF} \cong c(1 + \frac{\omega_p^2}{2\Omega^2})$. The nonresonant dielectric permittivity of the plasma for the XUV

radiation is, in turn, equal to unity due to the very high frequency of the XUV radiation, $\omega \gg \omega_p$, $c_{HF} \cong c$. Thus, the dispersion of plasma provides a mismatch of the phase velocities of the LF and the HF fields. As a consequence, the generated attosecond XUV radiation pulses are broadened by the value $\Delta\tau_{\text{pulse}} = \frac{L}{c_{HF}} - \frac{L}{c_{LF}} \cong \frac{2\pi N_e e^2 L}{m_e \Omega^2 c}$, equal to the time delay between the HF and the LF radiation components, acquired in the medium. In the above considered case of the Li^{2+} plasma ($N_{\text{Li2+}} = 10^{18}$ cm^{-1}, $N_e = 2 \times 10^{18}$ cm^{-1}, $L =$ 80 μm) irradiated by the 2-μm laser field, the broadening of the produced attosecond pulses in Figs. 7 and 8 equals $\Delta\tau_{\text{pulse}} = 480$ as. This broadening can be reduced below 100 as, via fivefold reduction of the propagation length or the concentration of Li^{2+} ions at the cost of decrease of the peak intensity of the pulses from $I_{\max} = 0.5I_0$ in Fig. 7 or $I_{\max} = 0.9I_0$ in Fig. 8 to $I_{\max} = 0.08I_0$ or $I_{\max} = 0.14I_0$, respectively, and decrease of the conversion efficiency from 12% to 2%. Another approach to reduce the dispersive pulse broadening relies on quasi-phase-matching [48,49]. Use of the quasi-phase-matching structure [49] would allow one to reduce the pulse broadening below 100 as without accompanying attenuation of the pulses and to produce the pulse trains, similar to those shown in Figs. 7 and 8. However, the most elegant way to eliminate the effects of plasma dispersion might be to adjust the phase velocity of the XUV radiation c_{HF} to the value of c_{LF} via appropriate detuning of the incident XUV radiation from the resonance.

IV. CONCLUSION

In conclusion, we have presented the analytical solution uncovering the origin of the ultrashort femto- and attosecond pulse formation from a near-resonant HF radiation in a hydrogenlike medium irradiated by a LF laser field with intensity far below the threshold for atomic ionization from the ground state [24,26]. We took into account quasistatic splitting of the excited atomic energy level into the sublevels, oscillating in space and time along with the LF field strength due to the linear Stark effect, as well as the constant shift and broadening of the atomic transition lines produced by the LF field via the quadratic Stark effect and the tunnel ionization from the excited states, respectively. The analytical solution is derived for an optically thin medium neglecting rescattering of the HF radiation. It shows that the possibility to produce ultrashort pulses [24,26] arises from constructive interference of the atomic coherencies, resonantly excited at the transitions from the ground energy level to the sublevels of the first excited level, split by the LF field, and interference of the scattered HF radiation with the incident one. We discussed the experimental possibilities to produce (i) 2.6-fs pulses from 122-nm VUV radiation in atomic hydrogen under the action of a 10.65-μm CO_2-laser field and (ii) 340-as pulses from 13.74-nm XUV radiation in the medium of Li^{2+} ions irradiated by a 2-μm laser field. The analytical solution is found to be in excellent agreement with the numerical calculation within the more general model, which takes into account the propagation effects in an optically deep medium as well as the space-time dependencies of both the nonlinear Stark shift and splitting of the excited atomic energy level and excited-state ionization rates [25,27]. The produced pulses are almost bandwidth limited. The pulse formation does not imply external adjustment of phases of the generated sidebands. The pulses can be produced either with attenuation of the output spectral component at the frequency of the incident radiation or without it. In the former case, the produced pulses are shorter, while in the latter case the peak intensity of the pulses is higher. The numerical solutions show that the peak intensity of the pulses can substantially exceed the intensity of the incident near-resonant radiation, while the conversion efficiency can reach dozens percent. We analyzed the role of plasma dispersion in the medium of Li^{2+} ions and showed that it does not prevent formation of attosecond pulses from the XUV radiation. Finally, the analytical solution derived in this paper shows robustness of the discussed approach to the ultrashort pulse formation from resonant radiation vs variation of major experimental parameters.

ACKNOWLEDGMENTS

We are grateful to Mikhail Emelin for fruitful discussions and to Mikhail Ryabikin for careful reading of the paper and useful remarks. This research was supported by RFBR, Grants No. 12-02-12101, No. 12-02-31325, No. 12-02-33074, and No. 13-02-00831; the Ministry of Education and Science of the Russian Federation, Contracts No. 8520 and No. 11.G34.31.0011; and NSF Grant No. 1307346. V.A.A. acknowledges support for young scientists from the Dynasty Foundation.

[1] A. H. Zewail, J. Phys. Chem. A **104**, 5660 (2000).
[2] T. Brabec and F. Krausz, Rev. Mod. Phys. **72**, 545 (2000).
[3] P. Agostini and L. F. DiMauro, Rep. Prog. Phys. **67**, 813 (2004).
[4] P. B. Corkum and F. Krausz, Nat. Phys. **3**, 381 (2007).
[5] F. Krausz and M. Ivanov, Rev. Mod. Phys. **81**, 163 (2009).
[6] P. Salières, A. Maquet, S. Haessler, J. Caillat, and R. Taïeb, Rep. Prog. Phys. **75**, 062401 (2012).
[7] S. Rausch, Th. Binhammer, A. Harth, J. Kim, R. Ell, F. X. Kärtner, and U. Morgner, Opt. Express **16**, 9739 (2008).
[8] S. Rausch, Th. Binhammer, A. Harth, F. X. Krtner, and U. Morgner, Opt. Express **16**, 17410 (2008).
[9] R. K. Shelton, L.-S. Ma, H. C. Kapteyn, M. M. Murnane, J. L. Hall, and J. Ye, Science **293**, 1286 (2001).
[10] T. R. Schibli, J. Kim, O. Kuzucu, J. T. Gopinath, S. N. Tandon, G. S. Petrich, L. A. Kolodziejski, J. G. Fujimoto, E. P. Ippen, and F. X. Kaertner, Opt. Lett. **28**, 947 (2003).
[11] G. Krauss, S. Lohss, T. Hanke, A. Sell, S. Eggert, R. Huber, and A. Leitenstorfer, Nat. Photonics **4**, 33 (2010).
[12] K. Yamane, Z. Zhang, K. Oka, R. Morita, M. Yamashita, and A. Suguro, Opt. Lett. **28**, 2258 (2003).
[13] E. Matsubara, K. Yamane, T. Sekikawa, and M. Yamashita, J. Opt. Soc. Am. B **24**, 985 (2007).
[14] K. Okamura and T. Kobayashi, Opt. Lett. **36**, 226 (2011).
[15] S. E. Harris and A. V. Sokolov, Phys. Rev. Lett. **81**, 2894 (1998).
[16] M. Y. Shverdin, D. R. Walker, D. D. Yavuz, G. Y. Yin, and S. E. Harris, Phys. Rev. Lett. **94**, 033904 (2005).

[17] W.-J. Chen, Z.-M. Hsieh, S. W. Huang, H.-Y. Su, C.-J. Lai, T.-T. Tang, Ch.-H. Lin, C.-K. Lee, R.-P. Pan, C.-L. Pan, and A. H. Kung, Phys. Rev. Lett. **100**, 163906 (2008).
[18] P. Antoine, A. L'Huillier, and M. Lewenstein, Phys. Rev. Lett. **77**, 1234 (1996).
[19] P. M. Paul, E. S. Toma, P. Breger, G. Mullot, F. Augé, Ph. Balcou, H. G. Muller, and P. Agostini, Science **292**, 1689 (2001).
[20] E. Goulielmakis, M. Schultze, M. Hofstetter, V. S. Yakovlev, J. Gagnon, M. Uiberacker, A. L. Aquila, E. M. Gullikson, D. T. Attwood, R. Kienberger, F. Krausz, and U. Kleineberg, Science **320**, 1614 (2008).
[21] S. Gordienko, A. Pukhov, O. Shorokhov, and T. Baeva, Phys. Rev. Lett. **93**, 115002 (2004).
[22] U. Teubner and P. Gibbon, Rev. Mod. Phys. **81**, 445 (2009).
[23] A. A. Gonoskov, A. V. Korzhimanov, A. V. Kim, M. Marklund, and A. M. Sergeev, Phys. Rev. E **84**, 046403 (2011).
[24] Y. V. Radeonychev, V. A. Polovinkin, and O. Kocharovskaya, Phys. Rev. Lett. **105**, 183902 (2010).
[25] V. A. Polovinkin, Y. V. Radeonychev, and O. Kocharovskaya, Opt. Lett. **36**, 2296 (2011).
[26] Y. V. Radeonychev, V. A. Polovinkin, and O. Kocharovskaya, Laser Phys. **21**, 1243 (2011).
[27] Y. V. Radeonychev, V. A. Polovinkin, and O. Kocharovskaya, Laser Phys. **22**, 1547 (2012).
[28] V. A. Antonov, Y. V. Radeonychev, and O. Kocharovskaya, Phys. Rev. Lett. **110**, 213903 (2013).
[29] E. V. Vanin, A. V. Kim, A. M. Sergeev, and M. C. Downer, JETP Lett. **58**, 900 (1993), http://www.jetpletters.ac.ru/ps/1195/article_18037.shtml.
[30] T. Brabec and F. Krausz, Phys. Rev. Lett. **78**, 3282 (1997).
[31] H. K. Avetissian, B. R. Avchyan, and G. F. Mkrtchian, Phys. Rev. A **74**, 063413 (2006).
[32] R. J. Damburg and V. V. Kolosov, in *Rydberg States of Atoms and Molecules*, edited by R. F. Stebbings and F. B. Dunning (Cambridge University Press, Cambridge, UK, 1983), pp. 31–72.
[33] V. A. Polovinkin, Ph.D. thesis, Institute of Applied Physics of the Russian Academy of Sciences, Nizhny Novgorod, Russia, 2012.
[34] O. J. Luiten, H. G. C. Werij, M. W. Reynolds, I. D. Setija, T. W. Hijmans, and J. T. M. Walraven, Appl. Phys. B **59**, 311 (1994).
[35] C. E. M. Strauss and D. J. Funk, Opt. Lett. **16**, 1192 (1991).
[36] V. V. Apollonov, P. B. Corkum, R. S. Taylor, A. J. Alcock, and H. A. Baldis, Opt. Lett. **5**, 333 (1980).
[37] H. T. Kim, I. W. Choi, N. Hafz, J. H. Sung, T. J. Yu, K.-H. Hong, T. M. Jeong, Y.-C. Noh, D.-K. Ko, K. A. Janulewicz, J. Tümmler, P. V. Nickles, W. Sandner, and J. Lee, Phys. Rev. A **77**, 023807 (2008).
[38] J. J. Rocca, Y. Wang, M. A. Larotonda, B. M. Luther, M. Berrill, and D. Alessi, Opt. Lett. **30**, 2581 (2005).
[39] C. Rajyaguru, T. Higashiguchi, M. Koga, K. Kawasaki, M. Hamada, N. Dojyo, W. Sasaki, and S. Kubodera, Appl. Phys. B **80**, 409 (2005).
[40] B. W. J. McNeil and N. R. Thompson, Nat. Photonics, **4**, 814 (2010).
[41] Free-electron laser FLASH, http://flash.desy.de/.
[42] Seeded free-electron laser FERMI@Elettra, http://www.elettra.trieste.it/FERMI/.
[43] X. Gu, G. Marcus, Y. Deng, T. Metzger, C. Teisset, N. Ishii, T. Fuji, A. Baltuška, R. Butkus, V. Pervak, H. Ishizuki, T. Taira, T. Kobayashi, R. Kienberger, and F. Krausz, Opt. Express **17**, 62 (2009).
[44] B. E. Schmidt, P. Béjot, M. Giguère, A. D. Shiner, C. Trallero-Herrero, É. Bisson, J. Kasparian, J.-P. Wolf, D. M. Villeneuve, J.-C. Kieffer, P. B. Corkum, and F. Légaré, Appl. Phys. Lett. **96**, 121109 (2010).
[45] F. Silva, P. K. Bates, A. Esteban-Martin, M. Ebrahim-Zadeh, and J. Biegert, Opt. Lett. **37**, 933 (2012).
[46] T. Harada, T. Hatano, and M. Yamamoto, in *Proceedings of the 8th International Conference on X-Ray Microscopy, "XRM 2005," Himeji, Japan, 2005*, edited by S. Aoki, Y. Kagoshima, and Y. Suzuki, IPAP Conf. Ser. **7**, 195 (2005).
[47] N. Kaiser, S. Yulin, M. Perske, and T. Feigl, *High-performance EUV Multilayer Optics, Advances in Optical Thin Films III*, edited by N. Kaiser, M. Lequime, and H. A. Macleod, Proc. SPIE **7101**, 71010Z (2008).
[48] C.-C. Kuo, C.-H. Pai, M.-W. Lin, K.-H. Lee, J.-Y. Lin, J. Wang, and S.-Y. Chen, Phys. Rev. Lett. **98**, 033901 (2007).
[49] A. Willner, F. Tavella, M. Yeung, T. Dzelzainis, C. Kamperidis, M. Bakarezos, D. Adams, M. Schulz, R. Riedel, M. C. Hoffmann, W. Hu, J. Rossbach, M. Drescher, N. A. Papadogiannis, M. Tatarakis, B. Dromey, and M. Zepf, Phys. Rev. Lett. **107**, 175002 (2011).